Dynamic MRI in indirect estimation of microvessel density, histologic grade, and prognosis in colorectal adenocarcinomas

N. Tuncbilek,[1] H. M. Karakas,[2] S. Altaner[3]

[1]Department of Radiology, Trakya University School of Medicine, 22030 Edirne, Turkey
[2]Department of Radiology, Faculty of Medicine, Inonu University, Trugut Ozal Medical Center, Malatya, Turkey
[3]Department of Pathology, Trakya University School of Medicine, 22030 Edime, Turkey

Abstract

The relations of dynamic contrast-enhanced magnetic resonance imaging (DCE-MRI) parameters to microvessel density (MVD), histologic grade, and presence of metastasis were evaluated to establish new prognostic indicators in colorectal cancer (CRC). Fast-low angle shot DCE-MRI parameters (time-intensity curves, TICs; maximal relative enhancement within the first minute, $E_{max/1}$; maximal relative enhancement of the entire study, E_{max}; steepest slope of the contrast enhancement curve; and time to peak enhancement) of 21 CRCs (seven Duke stage B, 12 Duke stage C, and two Duke stage D) were retrospectively evaluated and correlated with corresponding postoperative MVD measurements, histologic grades, and presence of metastasis at 2 years. TICs were classified as type A in nine (43%), type B in seven (33%), and type C in five cases (24%). There was a significant difference between TIC types with regard to MVD ($p < 0.05$–0.001). Time to peak enhancement, steepest slope of TIC, and $E_{max/1}$ were strongly correlated with MVD ($r = -0.765$, $p < 0.01$; $r = 0.681$, $p < 0.01$; $r = 0.634$, $p < 0.01$; respectively). MVD, steepest slope of the enhancement curve, $E_{max/1}$, and E_{max} strongly correlated with histologic grade ($r = 0.475$, $p < 0.05$; $r = 0.683$, $p < 0.01$; $r = 0.687$, $p < 0.01$; $r = 0.791$, $p < 0.01$; respectively). There was a significant difference between groups of patients with and without metastasis with regard to histologic grade ($p < 0.05$) and two of the DCE-MRI parameters ($p < 0.005$ for $E_{max/1}$ and $p < 0.05$ for time to peak enhancement). Discriminant analysis correctly predicted the metastatic occurrence at 2 years in 90.5% of cases using $E_{max/1}$ ($p < 0.001$). Histologic grade resulted in lower rates of discrimination (66.7%; $p < 0.05$). DCE-MRI parameters may help in the prediction of MVD and histologic grade in CRC and may be used to predict therapeutic outcome.

Key words: Colorectal cancer—Dynamic magnetic resonance imaging—Contrast enhancement—Angiogenesis—Microvessel density—Prognostic indicators

Colorectal cancer (CRC) is the second most common cancer in the United States and the most common cancer in the gastrointestinal tract [1]. Several factors have been evaluated in primary CRC for prognostic significance. Commonly used prognostic factors such as histologic grading and clinical staging do not always effectively predict therapeutic outcome [2].

Angiogenesis, the new capillary formation in tumoral tissue, is currently being evaluated as a prognostic indicator in several types of cancer [3–5]. The rationale behind this evaluation is that tumor growth beyond a milimeter in solid tissues cannot occur without vascular support [6–8]. Tumor angiogenesis is generally assessed by counting microvessel densities (MVDs). Being a direct technique, this assessment has a significant shortcoming because it depends on the availability of a postoperative tumoral tissue or an adequate biopsy material [9].

To help in therapeutic or surgical planning, indirect markers of angiogenesis, such as blood measurement of angiogenic factors and dynamic contrast-enhanced magnetic resonance imaging (DCE-MRI), recently have been used [9]. Being noninvasive and rapid, these techniques carry significant advantages over direct methods, and they may be used to monitor response to treatment in patients who had not undergone surgical removal of their tumors [9].

In this study, the relation of DCE-MRI enhancement parameters to MVD, histologic grade, and presence of metastasis were evaluated to provide new radiologic prognostic indicators in CRC.
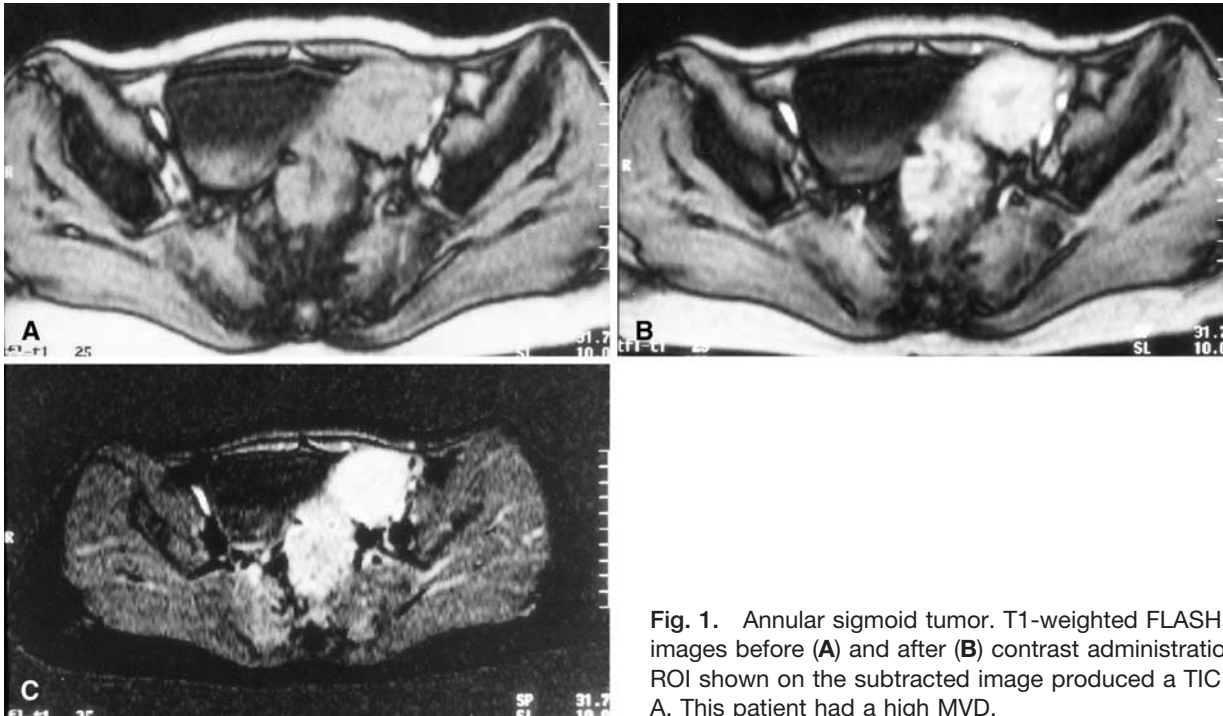
Correspondence to: N. Tuncbilek; *email:* drtuncbilek@hotmail.com

Fig. 1. Annular sigmoid tumor. T1-weighted FLASH images before (**A**) and after (**B**) contrast administration. **C** ROI shown on the subtracted image produced a TIC type A. This patient had a high MVD.

Materials and methods

The study group comprised 21 patients (12 male, nine female; age range = 30–72 years; mean = 54.3 years; standard deviation [SD] 11.2) consecutively referred to our MR unit with CRCs initially detected by barium enema ($n = 4$), computed tomography ($n = 8$), and colonoscopy ($n = 9$). The tumor was located in the rectum (eight cases), rectosigmoid colon (four cases), sigmoid colon (three cases), descending colon (one case), splenic flexure (one case), transverse colon (two cases), hepatic flexure (one case), and the cecum (one case). All cases were subsequently operated on and diagnosed as adenocarcinoma.

As part of their presurgical workup, all patients were investigated with a 1.0-T ($+/−20$ mT/m) superconductive scanner (Magnetom Impact Expert, Siemens, Erlangen, Germany). Conventional MR series (axial spin-echo T1, T2, and fat-suppressed T2 weighted) were used to locate tumoral lesions and to show their morphologic characteristics. After these preliminary series, a precontrast axial turbo fast low-angle shot (FLASH) sequence repetition time, 11 ms; echo time, 4.2 ms; NEX, 2; flip angle, 25°; band thickness, 163 kHz; slice thickness, 5 mm; matrix, 134 × 256; interslice gap, 1.5 mm) was applied to cover tumoral tissues (Figs. 1A, 2A, 3A).

After the precontrast turbo-FLASH sequence, patients received 0.1 mmol/kg gadopentetate dimeglumine (Gd-DTPA; Magnevist, Schering, Berlin, Germany) intravenously through a peripheral line at 5 mL/s using a power injector (Medrad Spectris, Maastricht, The Netherlands). In the postcontrast sequence, eight turbo FLASH series, each lasting 30 s, were performed sequentially in 4 min with identical parameters as those used for precontrast sequence (Figs. 1B, 2B, 3B). The onset for contrast injection and the data acquisition were triggered synchronously. Precontrast images were subtracted from the relevant postcontrast images to demonstrate differential tumoral enhancement.

Image analysis

Time-intensity curves (TICs)

TICs were produced automatically by using the scanner's software and baseline- (preenhancement) corrected signal intensity (SI) values of freely drawn region of interests (ROIs). For each tumor, one ROI for the most enhancing region was used. The ROIs covered areas of change between 0.3 to 0.4 cm^2. For each 30-s acquisition, the relevant SI data were treated automatically as acquired at the time the center of k-space was acquired. Therefore, SIs for 15 to 225 s with 30-s intervals were obtained.

In accord with Buadu et al. [10], TICs were classified into four different types depending on the basis of the results of a phase analysis of peak enhancement and washout of Gd-DTPA. In two of these types (A and B), peak enhancement was seen within the early or mid phase and was followed by a decrease or a plateau formation in the late phase (e.g., Figs. 1C, 2C). In the remaining two (C and D), enhancement was continuously increased throughout the study period or not seen at all, making the determination of the time to peak impossible (e.g., Fig. 3C).
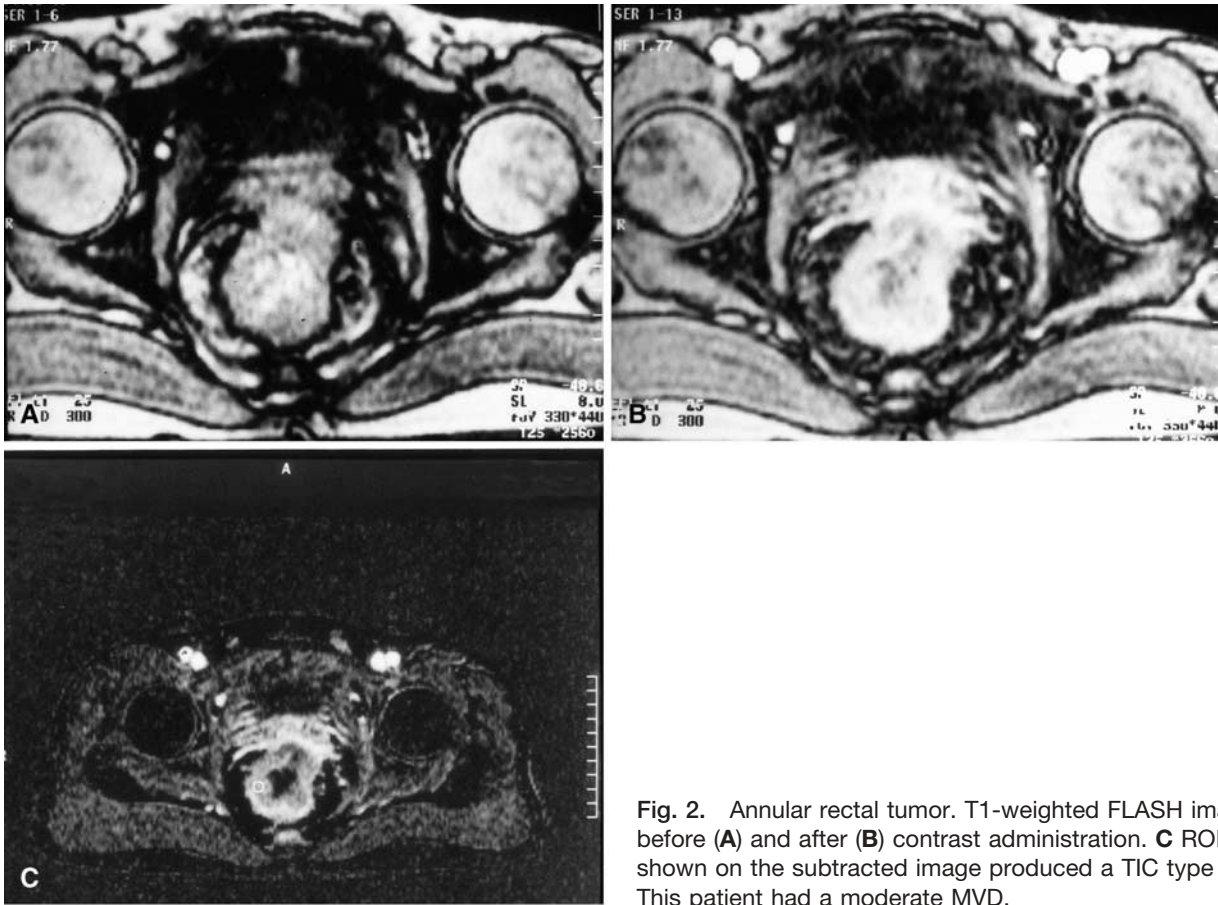
Fig. 2. Annular rectal tumor. T1-weighted FLASH images before (**A**) and after (**B**) contrast administration. **C** ROI shown on the subtracted image produced a TIC type B. This patient had a moderate MVD.
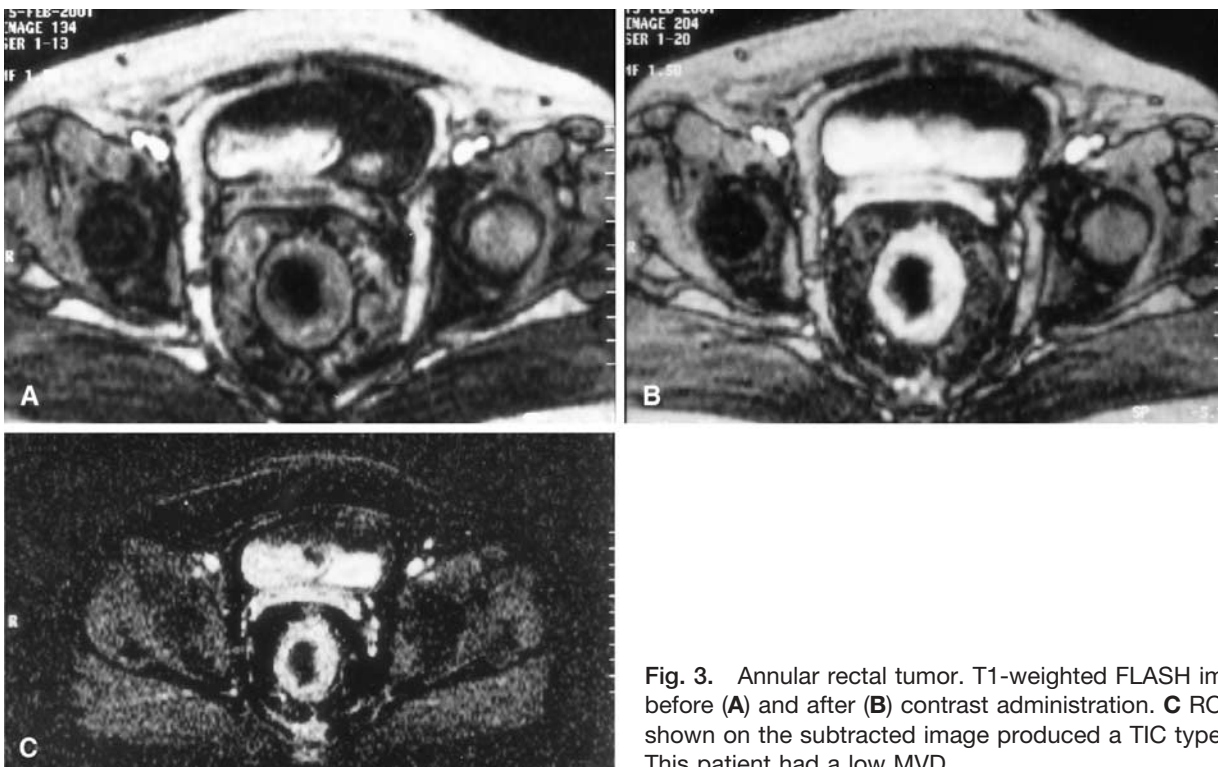

Fig. 3. Annular rectal tumor. T1-weighted FLASH images before (**A**) and after (**B**) contrast administration. **C** ROI shown on the subtracted image produced a TIC type C. This patient had a low MVD.

Enhancement parameters

The parameters were obtained with SI values of the above-defined ROIs. Maximal relative enhancement within the first minute ($E_{max/1}$) was expressed as the percentage of the nonenhanced SI by using the formula: $E_{max/1} = ([SI_{max/1} - SI_{pre/1}] \times 100)/ SI_{pre/1}$. In this formula, $SI_{max/1}$ represents the highest postcontrast SI reached within the first minute, and $SI_{pre/1}$ represents the relevant precontrast SI. Maximal relative enhancement of the entire study (E_{max}) was calculated with a similar formula. The steepest slope of the contrast enhancement curve was used as a measure of the tissue perfusion rate and expressed by the following equation, as defined by Buadu et al. [10]: steepest slope (%/s) = $([SI_{end} - SI_{prev}] \times 100)/ (SI_{pre} \times [T_{end} - T_{prev}])$, where prev indicates previous, and pre indicates precontrast. SI_{end} and SI_{prev} are the values on the contrast medium uptake curve that differed the most from image to image in the dynamic series. T_{end} and T_{prev} represent the time points corresponding to SI_{end} and SI_{prev}. Time to peak enhancement was defined as the postinjection time necessary to reach maximum SI.

The cardiac effects postulated to be negligible as semi-quantitative methods were used, and all subjects were within the normal ranges with regard to blood pressure and pulse rate. These parameters are less sensitive to changes in the arterial input function, which will have day-to-day variation, and may not be largely affected by changes in cardiac output [13]. The effect of the cardiac output therefore was not taken into consideration in the above-mentioned calculations.

Histopathologic analysis

After surgery each patient was assigned to one of the following stage groups according to the Duke classification [14] of resected tumors: seven (33%) Duke stage B, 12 (57%) Duke stage C, and two (10%) Duke stage D.

All cases were evaluated pathologically for histologic diagnosis and MVD determination. For each case a sample block containing tumoral and peritumoral tissue was chosen. Sections 4 μm thick were prepared from these blocks and immunostained with factor VIII–Related antigen-specific polyclonal antibody (DAKO, Glostrup, Denmark).

After identifying the most vascularized section and area in a low-power field (40×), vessels were counted in a high-power field (200×) with ocular grids. The section selected was macroscopically certified as being identical to the MR section in which SIs were measured. Any brown-stained endothelial cell or endothelial cell cluster that was clearly separate from adjacent microvessels, tumor cells, and other connective tissue elements was considered a single, countable microvessel. Vessel lumens, although usually present, were not necessary for a structure to be defined as a microvessel; red cells were not used to define a vessel lumen. Mean vessel numbers were calculated by averaging the number of defined vessels in the six most vascularized tumoral areas [3, 11, 12].

Follow-up of patients

All patients were followed in the postoperative period at our institution. At the end of 2 years postoperatively, all patients were alive. Ten had metastatic involvement, and the remaining patients were disease free.

Statistical analysis

The difference between multiple TICs and Duke stage groups with respect to MVDs were investigated with analysis of variance (ANOVA). Pearson moment correlation tests were performed to determine the strength of the relations between DCE-MRI parameters, MVD, and histologic grade. Differences between groups of patients with and without metastasis with respect to MVD, histologic grade, and DCE-MRI parameters were tested by using independent sample t test.

To build a predictive model of group membership based on observed characteristics of each case, a discriminant analysis was performed. Sets of discriminant functions based on linear combinations of the significant predictor variables providing the best discriminations between groups were generated with univariate ANOVA.

For all tests $p > 0.05$ was considered statistically significant. Larger values are indicated when relevant.

Results

MVDs were between 18 and 51 (mean = 28.2, SD = 8.1) in the 200X high-power field. ANOVA produced no statistically significant difference between Duke stages with respect to MVD. Histologically, eight patients had high-, six had medium-, and seven had low-grade tumors. There was a significant correlation between MVD and histologic grade ($r = 0.475$, $p < 0.05$).

TICs of the tumoral tissues were classified as type A in nine (43%), type B in seven (33%), and type C in five (24%) cases (Fig. 4). ANOVA produced a statistically significant difference between TIC types with regard to MVD (for types A and B: $p < 0.05$, for types A and C: $p < 0.001$, for types B and C: $p < 0.005$). The comparison of MVDs for different TIC types are presented in Figure 5.

Peak enhancement was reached between 45 and 225 s (mean = 117.86, SD = 58.15). The steepest slope of the enhancement curve was between 1.00 and 5.83 (mean = 2.97, SD = 1.77). The $E_{max/1}$ was 48 to 180 (mean = 97.14, SD = 37.39). Time to peak enhancement, steepest slope of TIC, and $E_{max/1}$ were very strongly correlated with MVD ($r = -0.765$, $p < 0.01$; $r = 0.681$, $p < 0.01$; $r = 0.634$, $p < 0.01$; respectively. Figs. 678). The E_{max} was between 61 and 180 (mean = 108.9, SD = 33.1). No significant correlation was found between this parameter and MVD. Steepest slope of the enhancement curve, $E_{max/1}$, and E_{max} were strongly correlated with histologic grade ($r = 0.683$, $p < 0.01$; $r = 0.687$, $p < 0.01$; $r = 0.791$, $p < 0.01$; respectively).
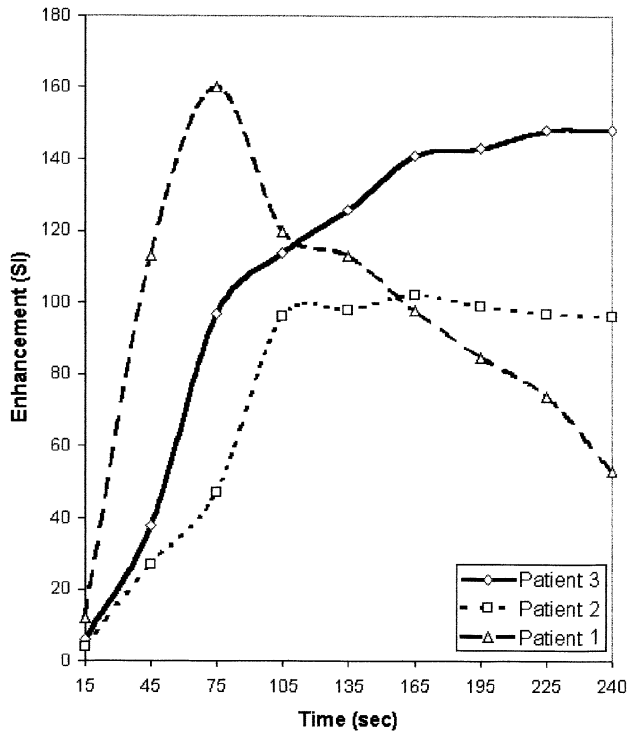
Fig. 4. Time-intensity curves for the patients presented in Figures 1–3.
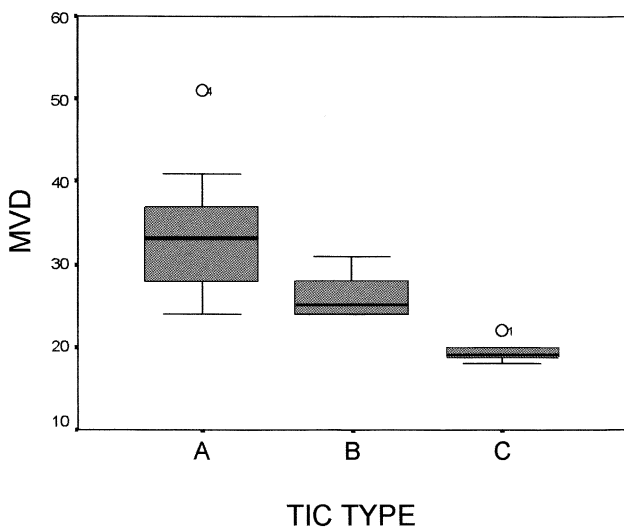
Fig. 5. The comparison of descriptive characteristics of MVDs for different TIC types.

Fig. 6. Scatter plot of the MVD versus time to peak enhancement ($r = -0.765$, $p < 0.01$).
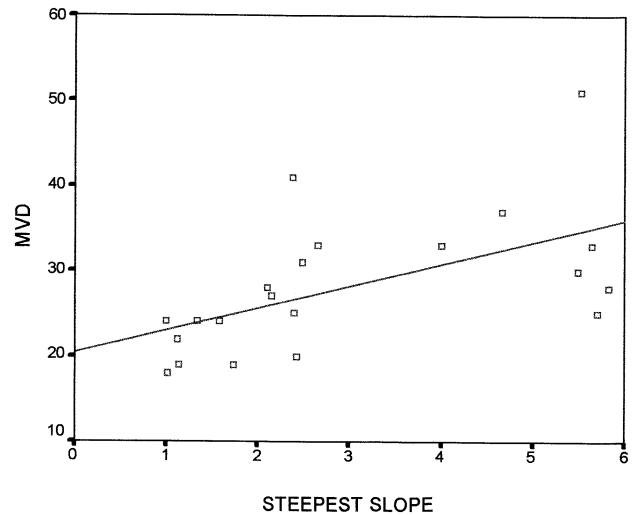
Fig. 7. Scatter plot of MVD versus the steepest slope of the enhancement curve ($r = 0.681$, $p < 0.01$).

Discriminant analysis correctly predicted the presence of metastasis at 2 years in 90.5% of cases when using $E_{max/1}$ ($p < 0.001$). Histologic grade and time to peak enhancement resulted in lower rates of discrimination (66.7%, $p < 0.05$, and 76.2%, $p < 0.05$, respectively).

Discussion

The importance of angiogenesis in tumor growth is well established [9]. The assessment of angiogenesis in clinical practice has relied mainly on immunostaining of postoperative specimens to count MVDs. Despite an international consensus on methodology for assessing MVD [15], there are variations in antibody usage and counting techniques. This has produced conflicting results, and it is unclear with

There was a statistically significant difference between patients with and without metastasis with regard to histologic grade ($p < 0.05$) and two of the DCE-MRI parameters ($p < 0.005$ for $E_{max/1}$ and $p < 0.05$ for time to peak enhancement). In contrast, MVD, steepest slope of the enhancement curve, and E_{max} did not produce a significant difference for presence of metastasis.
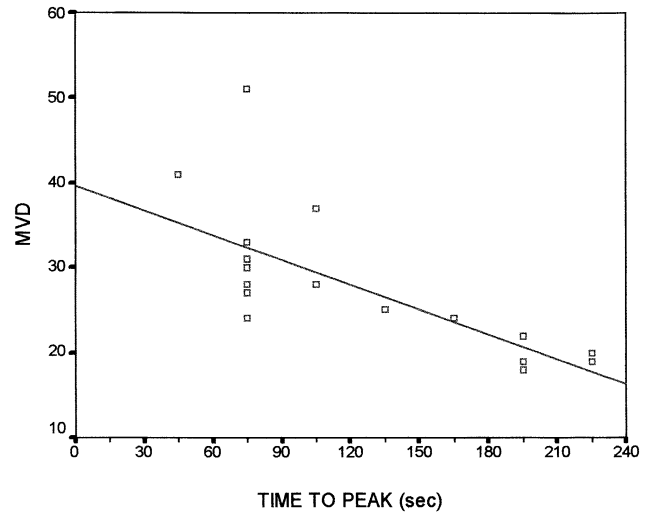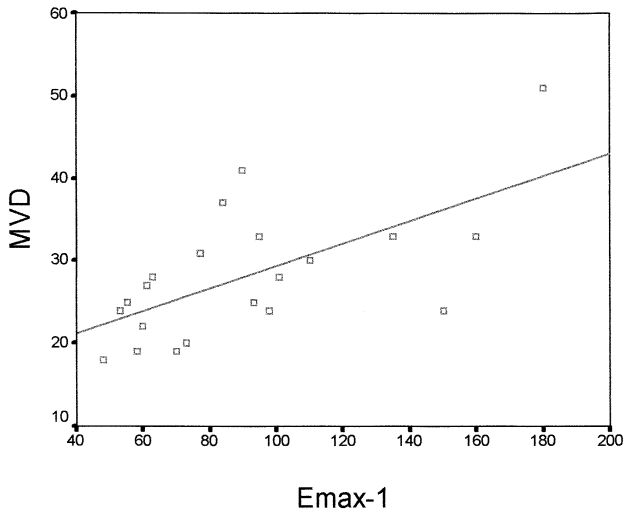
Fig. 8. Scatter plot of MVD versus maximal relative enhancement in the first minute ($E_{max/1}$; $r = 0.634$, $p < 0.01$).

respect to CRC whether high MVD is of reliable prognostic significance [16] or not [17–19]. This conflict is added to the main shortcoming of the technique, namely MVD calculation is dependent on the availability of a pathologic specimen [9].

DCE-MRI has proved to be accurate in the differentiation of benign scar from recurrence of soft tissue neoplasms and breast tumors [20, 21]. In CRC, the validity of this method was first demonstrated by Muller et al. [22] with a dynamic spin-echo sequence. This study was followed by another correlating DCE-MRI with tumoral perfusion index and serum level of vascular endothelial growth factors [9]. To date, no study was performed on CRC to correlate DCE-MRI with MVD. Such a correlation was studied only for breast cancer, resulting in mixed reports [10, 23–25]. Weidner and Folkman [8] recently reviewed the published reports that support or contradict the value of assessing tumor vascularity as a prognostic test in breast cancer patients. They suggested several explanations for observed associations between intratumoral MVD and various measures of tumor aggressiveness, including the suggestion that MVD within a tumor is probably a direct measurement of the size of the vascular window through which tumor cells pass to spread to distant sites [8]. This vascular window concept also could be used to support the hypothesis that MVD and DCE-MRI parameters may be associated.

The association between DCE-MRI and angiogenesis has a complex nature. Angiogenesis may be defined as the division rate of vascular cells or the spatial density of capillaries. In contrast, DCE-MRI measures represent complex interactions between specific blood flow, heterogeneity of flow, diffusion constants in the assessed tissues, spatial variability of these constants, and volumes of distribution of the enhancing agent [26]. In this study, spatial vessel density measured as MVD correlated strongly with the DCE-MRI

measures (time to peak enhancement, steepest slope of the enhancement curve, and $E_{max/1}$). There has been no previous study demonstrating such an association in CRC, but our findings are similar to those obtained in previous studies of MVD and DCE-MRI measures in breast carcinoma, thus supporting the vascular window concept of Weidner and Folkman [8].

The main impetus of the present study was to find prognostic information regarding the outcome of patients with CRC. The outcome is determined by tumor size, extent, stage, and biologic behavior [27]. Tumor behavior in turn is largely determined by its histologic grade. In our patients, histologic grades correlated strongly with DCE-MRI parameters and correctly predicted the metastasis at 2 years' follow-up in 66.7% of cases. $E_{max/1}$ resulted a much higher rate of prediction (90.5%), whereas MVD did not produced a significant classification with regard to outcome.

This study was based on the analysis of semiquantitative indices. Tofts et al. [28] recently developed a consensus of opinion about the standard quantities and symbols that should be adopted when using this technique to obtain fully quantitative parameters relating to tissue perfusion, microvessel permeability, and surface area. However, many groups still use semiquantitative indices. Relative changes in such semiquantitative parameters are indirectly related to changes in the physiologic endpoint of interest such as perfusion [29, 30]. The particular advantage of the semiquantitative analysis is that it is performed directly with the T1-weighted images, whereas quantitative analysis requires conversion of the MR signal intensities to Gd-DTPA concentrations [31]. Another advantage of the semiquantitative parameters lies within their good reproducibility [13]. Where measurement of relative changes in an individual or group of patients is required, simpler semiquantitative techniques are as reproducible as quantitative parameters [13]. Most of the semiquantitative parameters such as enhancement and initial area under the signal intensity–time curve for the first 90 s have good reproducibility within individuals, whereas many of the parameters such as K-trans ("transfer constant" for the transfer of contrast medium from the vessel into the extracellular extravascular space, EES) and K-ep (the "rate constant" for the transfer of contrast medium back from the EES into the vessel) are more variable [13]. Nevertheless, the parameters from the pharmacokinetic model are more easily related to the physiologic events in tissues and allow comparisons between reports from different institutions [13].

Due to the technical limitations of the study setting, the sampling interval was 30 s. Some investigators apply ultrafast studies to measure the first pass, whereas others prefer slower sequences with higher spatial resolution. The main disadvantage of an ultrafast study is that, when the dynamic study does not cover the entire lesion, there is a sampling error that can lead to misleading results [32]. If sensitivity to regions with rapid contrast kinetics is needed, contrast agent concentration in blood should be measured with 1 s of

temporal resolution; but techniques should be developed and validated to combine this with spatial resolution [33].

One of the limitations of this study was the use of SI values of freely drawn ROIs for the most enhancing region to determine the semiquantitative parameters. This method of evaluation of contrast enhancement is used in our and many other institutions where DCE-MRI is routinely performed [29]. Analyzing these parameters for each pixel rather than over the entire ROI does not dramatically affect the reproducibility [13]. However, tumors are characteristically heterogeneous and averaging MRI kinetic parameters over the entire tumor removes valuable information about this heterogeneity. Whether or not individual pixel analysis provides additional information for indirect estimation of MVD, histologic grade, and prognosis may be further evaluated in future studies.

In conclusion, various DCE-MRI parameters may help to predict MVD and histologic grades in CRC and may be used as the prognostic indicators of metastasis. By providing functional, in vivo data, DCE-MRI parameters may overcome some of the disadvantages of in vitro MVD studies that use anatomic data only and depend on the availability of pathologic specimens.

References

1. Readers JWAJ (2001) Neoplastic and inflammatory disease of the colon. Eur Radiol 11(suppl 2):105–126
2. DeVries AF, Griebel J, Kremser C, et al. (2001) Tumor microcirculation evaluated by dynamic magnetic resonance imaging predicts therapy outcome for primary rectal carcinoma. Cancer Res 15:2513–2516
3. Weidner N, Semple JP, Welch WR, Folkman J (1991) Tumor angiogenesis and metastasis-correlation in invasive breast carcinoma. N Eng J Med 324:1–8
4. Weidner N, Carroll PR, Flax J, et al. (1993) Tumor angiogenesis correlates with metastases in invasive prostat carcinoma. Am J Pathol 143:401–409
5. Maeda K, Chung YS, Takatsuka S, et al. (1995) Tumor angiogenesis as a predictor of recurrence in gastric carcinoma. J Clin Oncol 13:477–481
6. Rak JW, St Croix BD, Kerbel RS (1995) Consequences of angiogenesis for tumour progression, metastasis and cancer therapy. Anticancer Drugs 6:3–18
7. Folkman J, Merler E, Abernathy C (1970) Isolation of a tumor factor responsible for neovascularisation. J Exp Med 133:275–288
8. Weidner N, Folkman J (1996) Tumoral vascularity as a prognostic factor in cancer. In: DeVita VT, Hellman S, Rosenburg SA (eds) Important advances in oncology. Lippincott-Raven, Philadelphia, pp 167–190
9. George ML, Dzik-Jurasz AS, Padhani AR, et al. (2001) Non-invasive methods of assessing angiogenesis and their value in predicting response to treatment in colorectal cancer. Br J Surg 88:1628–1636
10. Buadu LD, Murakami J, Murayama S, et al. (1996) Breast lesions: correlation of contrast medium enhancement patterns on MR images with histopathologic findings and tumor angiogenesis. Radiology 200: 639–649
11. Matsubayashi R, Matsuo Y, Edakuni G, et al. (2000) Breast masses with peripheral rim enhancement on dynamic contrast-enhanced MR images: correlation of MR findings with histologic features and expression of growth factors. Radiology 217:841–848
12. Peters C, Medl M, Mirau M, et al. (1998) Color-coded and spectral doppler flow in breast carcinomas-relationship with the tumor microvasculature. Breast Cancer Res Treat 47:83–89
13. Galbraith SM, Lodge MA, Taylor NJ, et al. (2002) Reproducibility of dynamic contrast-enhanced MRI in human muscles and tumours: comparison of quantitative and semi-quantitative analysis. NMR Biomed 15:132–142
14. Johnson RD, Geisinger KR (1996) Colorectal adenocarcinoma: staging and histopathology. Semin Roentgenol 31:94–102
15. Vermeulen PB, Gasparini G, Fox SB, et al. (1996) Quantification of angiogenesis in solid human tumors: an international consensus on the methodology and criteria of evaluation. Eur J Cancer 32:2474–2484
16. Abdalla SA, Behzad F, Bsharah S, et al. (1999) Prognostic relevance of microvessel density in colorectal tumors. Oncol Rep 6:839–842
17. Choi HJ, Hyun MS, Jung GJ, et al. (1998) Tumor angiogenesis as a prognostic predictor in colorectal carcinoma with special reference to mode of metastasis and recurrence. Oncology 55:575–581
18. Takebayashi Y, Aklyama S, Yamada K, et al. (1996) Angiogenesis as unfavorable prognostic factor in human colorectal carcinoma. Cancer 78:226–231
19. Vermeulen PB, Van den Eynden GG, Huget P, et al. (1999) Prospective study of intatumoral microvessel density, p53 expression and survival in colorectal cancer. Br J Cancer 79:316–322
20. Erlemann R, Reiser MF, Peters PE, et al. (1989) Musculoskeletal neoplasms: static and dynamic Gd-DTPA-enhanced MR imaging. Radiology 171:767–763
21. Gilles R, Guinebretiere JM, Shapeero LG, et al. (1993) Assesment of breast cancer recurrence with contrast-enhanced subtraction MR-imaging: preliminary results in 26 patients. Radiology 188:473–478
22. Müller-Schimpfle M, Brix G, Layer G, et al. (1993) Recurrent rectal cancer: diagnosis with dynamic MR imaging. Radiology 189:881–889
23. Frouge C, Guinebretiere JM, Contesso G, Paola RD, Blery M (1994) Correlation between contrast enhancement in dynamic magnetic resonance imaging of the breast and tumor angiogenesis. Invest Radiol 29:1043–1049
24. Hulka CA, Simith BL, Sgroi DC, et al. (1997) Dynamic echo-planar imaging of the breast: experience in diagnosing breast carcinoma and correlation with tumor angiogenesis. Radiology 205:837–842
25. Axelsson K, Ljung BM, Moore DH, et al. (1995) Tumor angiogenesis as a prognostic assay for invasive ductal breast carcinoma. J Natl Cancer Inst 87:997–1008
26. Gribel J, Mayr NA, DeVries A, et al. (1997) Assessment of tumor microcirculation: a new role of dynamic contrast MR imaging. J Magn Reson Imaging 7:111–119
27. Bruckner HW, Pitrelli J, Merrick M (2000) Adenocarcinoma of the colon and rectum. Cancer Med 5:1472–1520
28. Tofts P, Brix G, Buckley D, et al. (1999) Estimating kinetic parameters from dynamic contrast-enhanced T(1)-weighted MRI of a diffusable tracer: standardized quantities and symbols. J Magn Reson Imaging 10:223–232
29. Hawighorst H, Libicher M, Knopp MV, et al. (1999) Evaluation of angiogenesis and perfusion of bone marrow lesions: role of semiquantitative and quantitative dynamic MRI. J Magn Reson Imaging 10:286–294
30. Bonnerot V, Charpentier A, Frouin F, et al. (1992) Factor analysis of dynamic magnetic resonance imaging in predicting the response of osteosarcoma to chemotherapy. Invest Radiol 27:847–855
31. Parker GJ, Suckling J, Tanner SF, et al. (1997) Probing tumor microvascularity by measurement, analysis and display of contrast agent uptake kinetics. J Magn Reson Imaging 7:564–574
32. Mirowitz SA, Totty WG, Lee JK (1992) Characterization of musculoskeletal masses using dynamic Gd-DTPA enhanced spin-echo MRI. J Comput Assist Tomogr 16:120–125
33. Evelhoch JL (1999) Key factors in the acquisition of contrast kinetic data for oncology. J Magn Reson Imaging 10:254–259